Enhancement of Photochemical Grafting of Terminal Alkenes at Surfaces via Molecular Mediators: The Role of Surface−Bound Electron Acceptors

ARTICLE *in* THE JOURNAL OF PHYSICAL CHEMISTRY C · APRIL 2008

Impact Factor: 4.77 · DOI: 10.1021/jp711167n

Enhancement of Photochemical Grafting of Terminal Alkenes at Surfaces via Molecular Mediators: The Role of Surface-Bound Electron Acceptors

Paula E. Colavita, Jeremy A. Streifer, Bin Sun, Xiaoyu Wang, Patrick Warf, and Robert J. Hamers*

Department of Chemistry, 1101 University Avenue, University of Wisconsin, Madison, Wisconsin 53706-1396

Received: November 25, 2007; In Final Form: December 21, 2007

The use of ultraviolet light to functionalize the surface of carbon-based materials with terminal alkenes has emerged as a way to overcome the high chemical stability of these surfaces to create functional interfaces. It was previously shown that surface-bound trifluoroacetic acid protected 10-aminodec-1-ene (TFAAD) can be used to promote the grafting of unreactive alkenes using 254 nm light, but the mechanism by which this enhancement occurs was not understood. Here, we present a detailed study of how surface-bound TFAAD enhances the grafting of organic molecules to the surface of hydrogen-terminated amorphous carbon. Infrared reflection absorption spectroscopy, X-ray photoelectron spectroscopy, scanning electron microscopy, and atomic force microscopy experiments show that pregrafting TFAAD onto carbon surfaces greatly enhances the subsequent grafting of 1-dodecene, dodecane and dodecane-d_{26} by locally facilitating photoemission of electrons. Using a photopatterned TFAAD "seed" layer, we demonstrate that subsequent grafting of these hydrocarbons is enhanced in regions immediately adjacent to the seed and proceeds almost exclusively parallel to the carbon surface. The roles of liquid-phase radical species, valence band holes, and the photochemical fragmentation of surface species in controlling the overall reaction mechanism are discussed.

1. Introduction

The use of ultraviolet light to functionalize carbon-based materials with terminal alkenes has emerged as a way to overcome the high chemical stability of these surfaces and create functional interfaces. Organic layers created via photochemical reaction of liquid *n*-alkenes using 254 nm light are particularly stable under a wide range of conditions because they are covalently linked to the carbon substrate through a C−C bond.[1,2] Photochemical grafting of molecular layers onto diamond,[1,3−7] amorphous carbon,[2,8] carbon nanofibers,[9] and glassy carbon[9,10] has been demonstrated using this procedure, and applications of these carbon/organic interfaces have been explored in the areas of sensors,[1,7,11] and energy conversion.[12,13]

We recently showed that grafting of molecular layers on hydrogen-terminated diamond[4,14] and amorphous carbon[8] is initiated by photoemission of an electron into the liquid alkene acceptor level.[4,8,14] These studies showed that the electron affinity of the alkene plays an important role in determining the reaction efficiency.[8,15] Furthermore, these results also led to the development of a practical approach to overcome the intrinsically low reactivity of some alkenes, by showing that a low coverage layer of a molecule that possesses a good electron acceptor (high electron-affinity group), a trifluoroacetamide-terminated alkene (trifluoroacetic acid protected 10-aminodec-1-ene, TFAAD), could greatly enhance the grafting of a second, less reactive, alkene.

In this work, we focus on investigating the mechanism by which the triflouroacetamide (TFA) group acts as a "molecular mediator" to enhance the reactivity of carbon surfaces. TFAAD serves as a model to understand whether the reactivity of semiconductor materials can be modulated by molecules that possess specific electronic properties. In the case of TFAAD on carbon, we find that the low-lying acceptor levels of the TFA group facilitate photoinduced charge transfer at the solid/liquid interface, thus promoting reactions between the semiconducting substrate and molecules in the liquid. Understanding what factors control the reactivity of the surface and what specific chemical/electronic molecular properties are important to promote chemical reactions, opens the possibility of rationally designing molecular mediators for semiconductor functionalization.

We have studied the structural and chemical changes of TFAAD layers grafted on hydrogen-terminated amorphous carbon induced by their photochemical reactions with 1-dodecene, dodecane, and dodecane-d_{26}. A combination of infrared reflection absorption spectroscopy (IRRAS), X-ray and ultraviolet photoelectron spectroscopy (XPS, UPS), scanning electron and force microscopy (SEM and AFM) has been used for this purpose. Our results show that TFAAD-terminated layers lead to grafting of not only unsaturated, but also saturated hydrocarbons, and that the final structure of the organic layer strongly depends on the electronic properties of the liquid phase. The surface-bound TFA groups can accept electrons and undergo dissociative decay, leading to the rapid loss of C−F bonds, or serve to facilitate electron transfer to acceptors in the liquid. Photoinduced electron transfer to molecular levels of chemisorbed TFAAD leads to the formation or highly reactive radical species. Carbon substrates can be chemically patterned using this photochemical approach; however, the sharpness of the resulting chemical boundaries is strongly dependent on the electronic properties of the liquid alkene. These results provide new insights into the role of electron photoemission in semiconductor photochemistry and on the role of electronic properties in the covalent attachment and growth of functional organic layers.

* Corresponding author. E-mail: rjhamers@wisc.edu.

10.1021/jp711167n CCC: $40.75
Published on Web 03/07/2008

2. Experimental Section

Chemicals. Electronic grade methanol (Fisher) and chloroform (Sigma Aldrich) were used without further purification. The following compounds were used for surface modification: trifluoroacetic acid protected 10-aminodec-1-ene (TFAAD, Chemical Synthesis Services), 1-dodecene 99% (Fluka), dodecane 99%, and dodecane-d_{26} 98% (Sigma Aldrich). All of the compounds were used as neat liquids; TFAAD was purified by vacuum distillation.

Sample Preparation. Amorphous carbon was sputter-coated using a DC magnetron system (Denton Vacuum) with a base pressure of $\leq 2 \times 10^{-6}$ Torr and an Ar pressure of 3 mTorr. The films were 50 nm thick and were deposited on two different types of substrates: (a) 100 nm evaporated titanium films on glass or silicon wafers for IRRAS measurements and (b) Ti-coated Mo foils for XPS. The amorphous carbon films were hydrogen-terminated in a 13.56 MHz inductively coupled plasma at H_2 pressure of 10 Torr for 10 min.

The H-terminated amorphous carbon samples were placed inside a nitrogen-purged reaction chamber sealed with a quartz window. A thin film of the neat alkene or alkane was placed on the substrates, a quartz slide was placed over the liquid to prevent evaporation, and the cell was illuminated with a low-pressure mercury lamp (254 nm, 4.9 eV photon energy, 15 mW/cm^2). After the reaction, samples were sonicated in chloroform and methanol and dried under nitrogen.

Characterization. IRRAS spectra were collected on a Fourier transform IR (FTIR) spectrometer (Bruker Vertex 70) equipped with a VeeMaxII variable angle specular reflectance accessory and a wire grid polarizer. The 100 nm thick Ti underlayers enhanced the reflectance of the sample and controlled the surface selection rules.[16] Spectra were collected using p-polarized light at 80° incidence from the surface normal; 500 scans at 4 cm^{-1} resolution were collected for both background and sample. A H-terminated amorphous carbon sample was used as a background in all cases. Typical root-mean-square (rms) and peak-to-peak noise levels were below 2×10^{-5} and 1×10^{-4} absorbance units, respectively.

XPS characterization was performed on an ultrahigh vacuum (UHV) system with 8×10^{-10} Torr base pressure equipped with a monochromatized Al K_α source (1486.6 eV nominal energy) and a multichannel array detector. Spectra were recorded with an analyzer resolution of 0.1−0.2 eV at a 45° takeoff angle. Atomic area ratios were determined by fitting absorption peaks to Voigt functions (Igor Pro) after Shirley background correction,[17] and normalizing the peak area ratios by the corresponding atomic sensitivity factors (C = 0.296; N = 0.477; O = 0.711; F = 1.0).[18] UPS characterization was carried out using a He(I) emission lamp (21.2 eV) and analyzer resolution of 0.05−0.1 eV. The sample was oriented at a takeoff angle of 75° (from the surface plane) and biased −4.50 to −9.00 V with respect to the spectrometer; this ensures that the sample vacuum level is higher in energy than that of the analyzer. Spectra at progressively higher biases were collected until the high binding energy cutoff was observed to converge; the spectrum thus obtained was used for the work function calculations. Energies are referenced to the sample Fermi level, determined by measurement of Ta clips directly in contact with the sample.

Patterning Experiments. A chromium mask having features on the ∼1 μm length scale was used to pattern the surfaces of hydrogen-terminated amorphous carbon. The mask was fabricated using electron-beam lithography to pattern a photoresist spin-coated on a fused quartz substrate. A 70 nm Cr film was deposited using an e-beam evaporation source followed by the "lift-off" of the remaining photoresist.

Photopatterned amorphous carbon samples were imaged using a Multimode, Nanoscope IV AFM (Veeco). Images were obtained in tapping mode using tips with nominal 3.5 N/m spring constant (NSC18, Mikromasch) at approximately 0.85 tapping ratios. Height images were flattened using a straight line prior to analysis. The thickness was measured by fitting straight lines to height profiles (averaged over 4 μm along step edges) before and after a step, followed by a calculation of the thickness at the midpoint of the dropping edge. Photopatterned samples were also imaged via SEM using a Leo Supra55 VP scanning electron microscope. Images were obtained as described in our previous work,[15] using 2 kV incident electron energy, the standard in-lens detector, and a typical working distance of 10−11 mm.

3. Results

Grafting of Hydrocarbons on TFAAD-Terminated Carbon. In our previous work, we showed that TFAAD readily grafted to H-terminated amorphous carbon, but surprisingly we found that other alkenes such as 1-dodecene showed very little grafting under identical conditions.[8] FTIR data further supporting this can be found in Supporting Information. Yet, we found that by pregrafting a partial layer of TFAAD, the grafting of 1-dodecene and other less reactive alkenes to H-terminated amorphous carbon could be greatly enhanced.[8] Thus, TFAAD acts as a seed layer that is able to enhance the grafting of other molecules to the surface. We proposed that the ability of TFAAD to enhance grafting was associated with the TFA groups, which are good electron acceptors. We also found evidence for some degradation of the TFA group, but the possible impact of this process on the reaction mechanism was not identified.

To address these questions, we conducted experiments to investigate the fate of the TFA group when subsequent photochemical reactions were carried out on TFAAD-terminated carbon and to determine whether these reactions required the presence of an unsaturated C═C bond. Figure 1(a) shows the typical IRRAS spectrum of a hydrogen-terminated carbon sample grafted with TFAAD for 15 h. Also shown are IRRAS spectra of samples prepared in this way that were subsequently reacted with 1-dodecene and with dodecane. The infrared peaks and assignments of TFAAD layers on hydrogen-terminated carbon have been discussed previously.[2,8] Briefly, the IRRAS spectrum displays the characteristic signature of an alkyl chain with methylene C−H stretching modes at ∼2933 and 2858 cm^{-1} and bending modes at 1466 and 1450 cm^{-1}. The amide I (C═O stretching) and II peaks at 1709 and 1564 cm^{-1} and C−F stretching modes in the region 1260−1120 cm^{-1} indicate the presence of a TFA-protecting group. After 15 h of illumination in the presence of 1-dodecene or dodecane, the characteristic TFA spectroscopic signature decreases in intensity; the carbonyl and C−F stretching vibrations decrease by ∼30% when the sample is reacted with 1-dodecene and completely disappear in the case of dodecane. The intensity of the CH_2-associated modes increases during these reactions; an estimate of the relative coverages of these organic layers can be obtained by integrating the absorption intensities in the C−H stretching region, assuming that orientation effects are negligible in the IRRAS signal. The total integrated area of the methylene-stretching modes increases by 60% when 1-dodecene is grafted onto the initial TFAAD-modified surface and increases by 30% for dodecane. These data suggest that the molecular layer has increased its coverage by ∼50%. In the case of dodecane, a

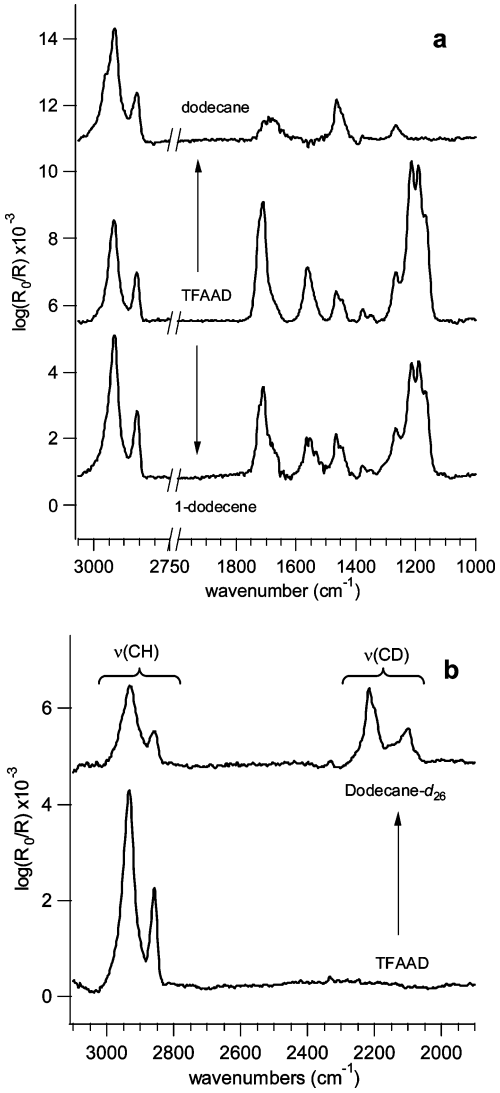

Figure 1. IRRAS spectra of organic layers grafted on amorphous carbon surfaces. (a) A TFAAD-terminated sample is subsequently grafted with 1-dodecene and dodecane. Although in both cases the hydrocarbons react with the surface, the spectral signature of the initial surface bound molecule is affected to a different extent. (b) IRRAS spectrum of a TFAAD-terminated sample after its reaction with dodecane-d_{26}, a fully deuterated alkane. The reaction involves fragmentation of the hydrocarbon backbone of the initial surface-bound molecule. Spectra were baseline corrected and offset for clarity.

prominent shoulder at 2952 cm^{-1} appears, which we assign to a methyl-stretching vibration. Control experiments performed on bare H-terminated amorphous carbon surfaces showed no detectable grafting for either 1-dodecene or dodecane in the absence of TFAAD (see Supporting Information).

To understand whether only the TFA groups or also the initially present hydrocarbon chains undergo chemical changes under UV illumination, we carried out experiments using dodecane-d_{26}, a fully deuterated alkane. Figure 1b shows the spectra of the initial TFAAD layer and that of the same sample after 15 h reaction time with dodecane-d_{26} under 254 nm light. The infrared spectrum shows a decrease in intensity of the C−H stretching peaks (2933 and 2858 cm^{-1}) and the appearance of C−D stretching peaks 2216 and 2100 cm^{-1}. These changes demonstrate that the C−H bonds are partially substituted by C−D bonds. An estimate of the coverage obtained by integrating the C−H and C−D stretchings (corrected by a factor of ∼1.9 to account for the difference in reduced mass)[19] yielded an increase by a factor of 1.4 compared to the initial TFAAD layer. This value is in good agreement with the factor of 1.3 increase in infrared absorbance of the CH_2 vibrations obtained when a TFAAD layer is exposed (under UV illumination) to hydrogenated dodecane.

In summary, these results show that surface-bound TFAAD enhances the subsequent photochemical reactivity of saturated as well as unsaturated molecules. The grafting experiments carried out using hydrogenated and deuterated molecules show that there is both some fragmentation of the TFA terminal group and of the backbone chain during this process. During photochemical reactions on TFAAD-terminated carbon, the organic layer increases its coverage by similar amounts for all three molecules tested. Surprisingly, however, the extent of TFA photodegradation is highly dependent on the specific molecule used.

Photodegradation of the TFA Group. To better quantify the extent of TFA photodegradation in different liquid environments, we characterized TFAAD-terminated carbon samples using XPS after their reaction in different environments as a function of time. Figure 2a shows survey spectra of TFAAD-terminated amorphous carbon samples (15 h reactions) that were then subjected to an additional photochemical reaction with dodecane for 0, 5, and 15 h. The surveys display absorption peaks that correspond to C(1s), N(1s), O(1s), and F(1s) photoionizations typically found for TFAAD-terminated samples.[2,3] The TFA group contains F, O, and N atoms in a ratio of 3:1:1; the area ratios $A_{F(1s)}/A_{O(1s)}/A_{N(1s)}$ of the F(1s), O(1s), and N(1s) peaks (after sensitivity factor correction) should therefore reflect this ratio in the case of intact TFA groups. The survey spectra show that this ratio is significantly altered after the TFAAD-modified sample is illuminated for progressively longer times in dodecane: the initial value of 3.2:1.3:1.0 falls to 2.0:1.3:1.0 after 5 h and to 1.1:1.5:1.0 after 15 h illumination time, strongly suggesting that C−F bonds are lost faster than C═O and C−N bonds.

Similar measurements were also carried out on TFAAD samples in 1-dodecene and on a TFAAD sample in UHV; the UHV experiment was carried out at a pressure of 1×10^{-9} Torr while illuminating the sample through a quartz window. Figure 2b shows the $A_{F(1s)}/A_{N(1s)}$ and $A_{F(1s)}/A_{C(1s)}$ ratios as a function of reaction time for TFAAD-modified samples subsequently illuminated while in contact with 1-dodecene with dodecane and in a UHV environment. Both the $A_{F(1s)}$:$A_{C(1s)}$ and $A_{F(1s)}$:$A_{N(1s)}$ ratios decrease upon illumination, and the decrease becomes faster going from 1-dodecene to dodecane to vacuum. A decrease in $A_{F(1s)}$:$A_{C(1s)}$ can result from a combination of TFA photodegradation (decrease in $A_{F(1s)}$) and hydrocarbon chain grafting (increase of $A_{C(1s)}$). On the other hand, a decrease in $A_{F(1s)}$:$A_{N(1s)}$ reflects exclusively the photodegradation of the TFA group. The observed decay rates indicate that the environment surrounding the chemisorbed TFAAD layer strongly influences the rate of photodegradation.

The above results show that the photodegradation process involves fragmentation of the TFA group, and that the C−F bonds are the most susceptible to cleavage in the TFA group. These results are in agreement with typical decay pathways for trifluoroacetamide radical anions, which are known to proceed through the loss of C−F bonds.[20−22] However, a remarkable difference in the rate of photodegradation is observed depending on whether the TFAAD-modified surface is in contact with 1-dodecene or dodecane, two structurally similar molecules. This suggests that the electronic properties of the liquid phase might

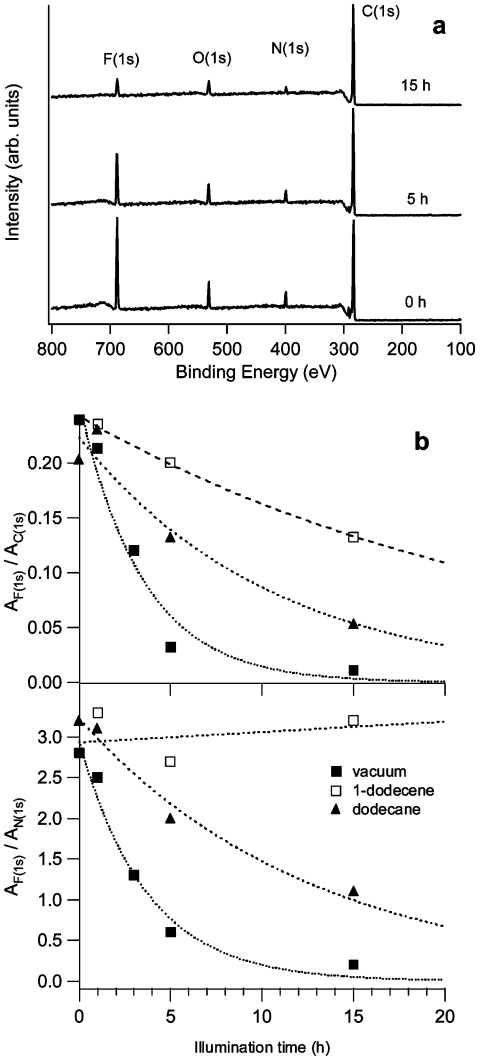

Figure 2. Photodegradation of the TFA terminal group followed by XPS. (a) Survey spectra obtained after illuminating a TFAAD-terminated sample with 254 nm light, for 0, 5, and 15 h while in contact with dodecane. (b) $A_{F(1s)}/A_{N(1s)}$ and $A_{F(1s)}/A_{C(1s)}$ ratios obtained after illuminating TFAAD-terminated samples in contact with 1-dodecene (□) and dodecane (▲) and in vacuum (■). An exponential decay has been fitted to the data to guide the eye.

play an important role in determining the fate of surface-bound TFA groups.

Electronic Properties of TFAAD-Terminated Surfaces. In our previous work, we observed that the photochemical reactivity of bare carbon surfaces toward different molecules depended on the electronic structure of both surface and molecule; photoemission of electrons from the carbon into liquid alkene acceptor levels was a key step in these reactions.[8] We therefore investigated via UPS whether photoemission is a viable process at TFAAD-terminated carbon surfaces under our reaction conditions, by measuring the work function in vacuum.

Figure 3 shows the He(I) UPS spectrum of a TFAAD-terminated amorphous carbon. The spectrum profile is markedly different from that of the bare sample[8] and is similar to that of TFAAD-terminated diamond reported by Nichols et al.[4] To measure the work function, the sharp cutoff in electron emission at high binding energy was fit to a line and extrapolated to zero intensity (see inset); this value was then subtracted from the incident photon energy (21.2 eV) to yield the work function.[23,24] The resulting value was 3.2 eV; this is 0.8 eV lower than the

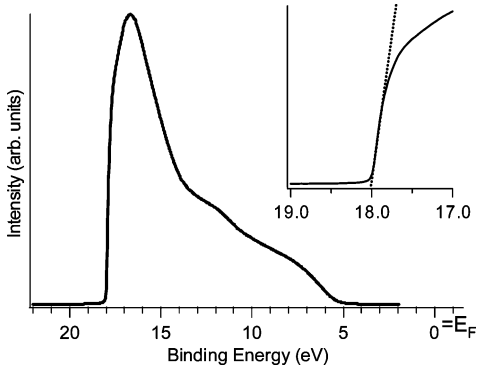

Figure 3. UPS spectrum of the TFAAD-terminated sample obtained after reaction of a hydrogen-terminated surface with TFAAD for 15 h. The inset shows details of the high-binding edge threshold and the linear fit used to determine the surface work function.

4.0 eV work function of the hydrogen-terminated surfaces.[8] The minimum energy barrier to photoemission is therefore smaller on TFAAD-terminated carbon than on hydrogen-terminated carbon, and both are smaller than the 4.9 eV photon energy used during functionalization.

Photopatterned Grafting of Molecules to Amorphous Carbon. Photochemical functionalization provides a pathway to preparing chemically patterned surfaces. However, the ability to do so is strongly dependent on the mechanism of the functionalization. We therefore investigated to what extent an initial surface pattern of TFAAD would be preserved after subsequent reactions to gain insights into what factors control the reaction at TFAAD-terminated surfaces. In these experiments, we used the Cr-on-quartz mask to control the spatial distribution of light hitting the carbon surface (with a thin film of TFAAD between the mask and the carbon surface) and investigated how the TFAAD patterns were modified by subsequent reactions.

Figure 4a,c shows typical AFM height images of chemically patterned substrates. Figure 4a shows a TFAAD chemical pattern where the dark areas correspond to regions that were not illuminated (and therefore consist of H-terminated carbon) and the brighter background corresponds to regions that were illuminated (and therefore are TFAAD-terminated carbon). Figure 4b displays an average height profile measured along the edge of this feature showing the sharp drop-off between functionalized and H-terminated regions; the height of the TFAAD layer obtained after 15 h of illumination is 5.1 ± 0.4 nm, with a roughness very close to that of the starting H-terminated surface (standard deviation $\sim 2.0 \pm 0.2$ nm). Because the height of a TFAAD monolayer is 1.5 nm,[5] the observed layer thickness of 5.1 nm shows that the grafting of TFAAD does not terminate after the first layer, but forms a thicker layer corresponding to approximately three molecular layers, in agreement with recent work on H-terminated diamond.[5,14]

TFAAD-patterned samples, such as the one shown in Figure 4a, were subsequently exposed to dodecane or 1-dodecene over their entire surface and illuminated with 254 nm light for 15 h. While we anticipated that these secondary exposures would graft these molecules (especially 1-dodecene) into the previously nonfunctionalized regions and thereby greatly reduce the spatial pattern produced by the original TFAAD, we found that the photomask features were still easily observed by AFM. Figure 4c shows the result obtained for the two-step grafting process carried out using 1-dodecene. The sharp height change of the

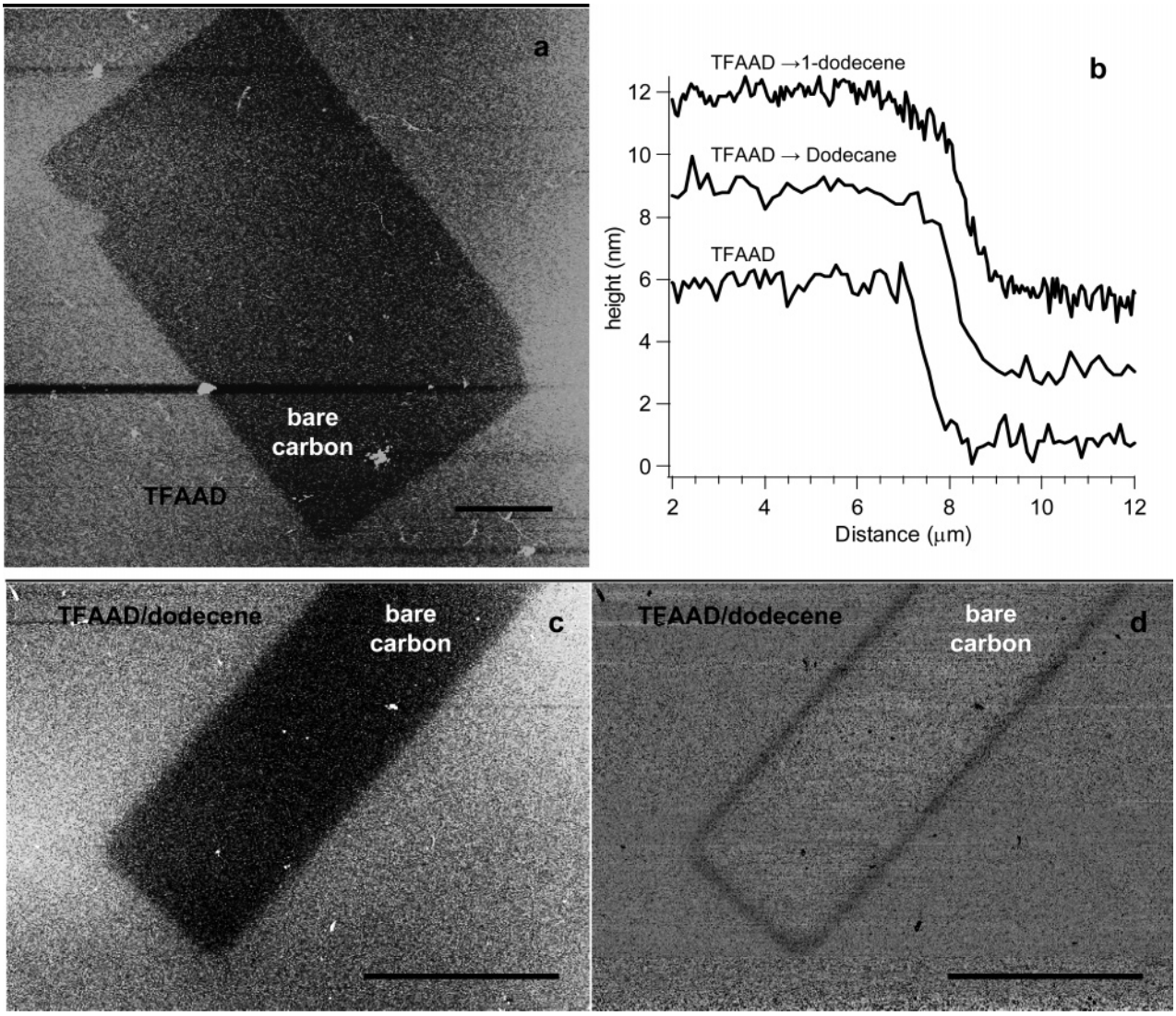

Figure 4. AFM images of chemical patterns on hydrogen-terminated amorphous carbon. The scale bars on the images correspond to 10 μm. (a) Pattern of TFAAD molecules on carbon: TFAAD-functionalized regions appear higher (brighter) than bare H-terminated carbon (dark). (b) Average height profiles for three photopatterned samples: TFAAD, TFAAD followed by dodecane, and TFAAD followed by 1-dodecene. The profiles have been offset for clarity. (c) Pattern obtained by grafting 1-dodecene over the entire area of a TFAAD-patterned carbon. (d) Phase image corresponding to the height image in panel c.

original TFAAD layer can still be easily observed. Figure 4b shows average height profiles for the three samples; grafting of TFAAD followed by dodecane yields a height change of 6.1 $\pm$ 0.3 nm across this step, while grafting of TFAAD followed by 1-dodecene yields a height change of 6.0 $\pm$ 0.3 nm. In these measurements, the center of the pattern (far from the edge) was used as the point of reference for the height changes; because neither 1-dodecene nor dodecane grafts effectively to carbon in the absence of TFAAD, the surface regions corresponding to the center of the dark regions are expected to be comprised of H-terminated carbon. Thus, the data suggest that the secondary grafting of 1-dodecene and dodecane onto the TFAAD regions leads to an additional increase of $\sim$1 nm in thickness of the TFAAD regions, while the lateral growth extends approximately 1 μm.

Close analysis of the AFM images reveals subtle but important differences in the width and sharpness of the patterns. The AFM profiles of the TFAAD-seeded dodecane and 1-dodecene patterns (Figure 4b) show that the transition from hydrogen-terminated to functionalized regions is more gradual than it is in the initial TFAAD pattern. The influence of imaging conditions on AFM topographic profiles makes it difficult to quantify these differences. However, this change in the sharpness of the patterns is also observed by scanning electron microscope analysis (vide infra). A second important difference is in the width of the molecular patterns. The sequential grafting of TFAAD followed by dodecane yields a pattern that closely replicates the initial TFAAD pattern with a nearly constant phase shift (of the AFM cantilever) over the entire image. However, the sequential grafting of TFAAD followed by 1-dodecene leads to changes in the feature sizes: the dark regions in Figure 4c that correspond to nonfunctionalized regions of the sample shrink from their original width of 9 to 7 μm, strongly suggesting that the 1-dodecene layer grows laterally starting at the edges of the TFAAD layer. This conclusion is further supported by the AFM phase image shown in Figure 4d. The phase image shows that grafting of 1-dodecene onto the TFAAD-patterned surface leads to the appearance of a dark stripe $\sim$1 μm in width separating the central region (which was not functionalized with TFAAD) from the outer region (which was functionalized with TFAAD). This stripe corresponds to a local region with a phase lag that is smaller than that on the adjacent regions. This result

appears to be consistent with previous studies showing that under light tapping-mode imaging conditions similar to those used here (high amplitude ratio and relatively soft cantilevers), the phase lag of CF_3-terminated layers is larger than that of CH_3-terminated layers due to increased energy dissipation associated with adhesive interactions.[25,26] We note that the IRRAS and XPS data on nonpatterned surfaces show that after sequential grafting of TFAAD followed by 1-dodecene, fluorinated groups are still present in the organic layer after 1-dodecene grafting (see Figure 1a). Consequently, we anticipate that in the patterning experiments, the regions originally functionalized with TFAAD will have some 1-dodecene embedded and form a mixed layer, while the advancing reaction front visible in AFM is expected to consist exclusively of alkyl chains. Thus, the AFM height data and phase data are both consistent with the presence of a two-dimensional reaction front forming in which the 1-dodecene layer grows laterally from the edge of the TFAAD functionalized regions.

The chemical photopatterns on amorphous carbon were also imaged with SEM; Figure 5a shows the surface of an amorphous carbon sample after photochemically patterning TFAAD for 15 h. The dark areas correspond to regions of bare H-terminated carbon, while the brighter background consists of TFAAD-terminated carbon. Because the in-lens detector used for SEM imaging primarily detects low-energy secondary electrons,[27,28] the observed contrast indicates that TFAAD layers increase the secondary electron yield compared with H-terminated carbon. Profiles of the secondary electron emission intensity measured over different edge regions revealed that the change in intensity from H-terminated to TFAAD-functionalized regions occurs within 0.3 ± 0.1 μm (measured as the distance over which the intensity changes from 10 to 90% of the constant value on each side).

SEM measurements confirmed the changes in feature sizes observed in AFM. Figure 5a shows a H-terminated carbon sample that was patterned with TFAAD as described earlier. Figure 5b,c shows SEM images of samples that were first patterned with TFAAD and then covered with either dodecane or 1-dodecene, respectively and (in both cases) illuminated for 15 h under 254 nm light over their entire area. Figure 5d shows typical intensity profiles at the pattern edge for the three samples discussed. The SEM image in Figure 5b of the TFAAD/dodecane sample shows features with sharp edges, characterized by an abrupt change in intensity that occurs within 0.5 ± 0.1 μm, demonstrating that only a marginal loss of sharpness results from this reaction. In contrast, Figure 5c of the TFAAD/1-dodecene sample shows a significant loss in sharpness under otherwise identical conditions. The contrast sharpness at functionalized/bare boundaries significantly worsens, and its determination becomes more difficult to quantify exactly: the edge drop-off occurs over 3 ± 1 μm.

An even more interesting result of the sequential grafting of TFAAD followed by 1-dodecene (Figure 5c) is that the dark (H-terminated) regions are reduced in size by approximately 1 μm at each edge compared with the original TFAAD-modified surface (Figure 5a) while the brighter regions are wider. These changes are in agreement with the AFM data, suggesting that the 1-dodecene molecules preferentially graft onto the H-terminated carbon regions immediately adjacent to the TFAAD regions, leading to a preferential reduction in size of the dark H-terminated regions. Additionally, the SEM image shows a line of higher intensity, approximately 1 μm wide, which appears to outline the entire border of the dark regions of nonfunctionalized carbon.

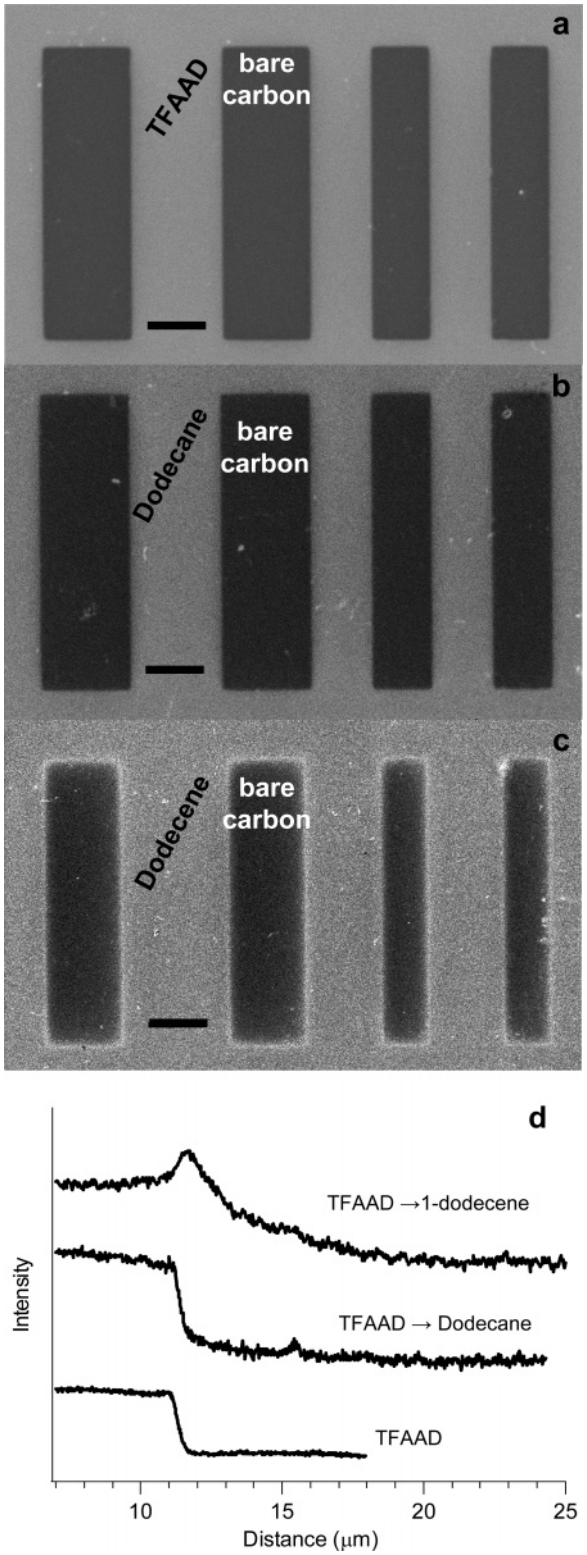

Figure 5. SEM images of chemical patterns on hydrogen-terminated amorphous carbon. The scale bar corresponds to 10 μm. (a) Pattern of TFAAD molecules (bright) on carbon (dark). (b) A pattern analogous to that on (a) after photochemical reaction with dodecane over the entire sample surface. (c) Pattern obtained after reaction with 1-dodecene over the entire area of a TFAAD-patterned sample. (d) Intensity profiles for pattern edges of samples in panels a, b, and c. The profiles have been shifted and offset to facilitate comparison.

The origin of the bright edge is particularly intriguing. In previous work, we investigated the contrast mechanism for diamond functionalized with different molecules[15] and showed

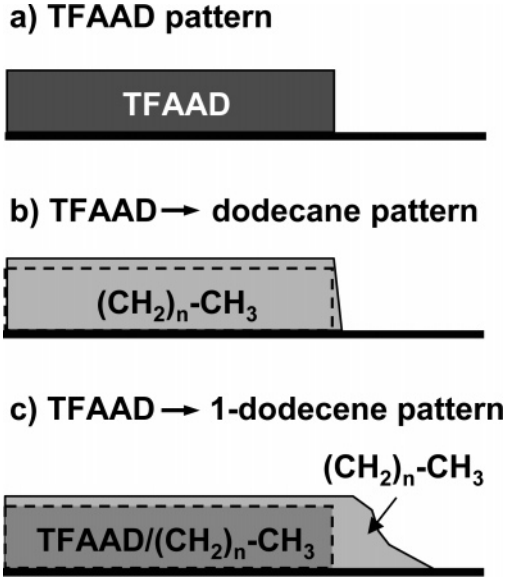

Figure 6. Chemical pattern composition and contrast as inferred from IRRAS, XPS, and scanning microscopies. In panels b and c, the original TFAAD layer is shown with dashed lines. The normal and lateral growths of the organic layer are shown on different scales to improve the clarity.

that molecules with acceptor levels lying above the vacuum level displayed higher electron yields and therefore appeared brighter in the SEM, while those with lower-lying acceptor levels appeared darker, in agreement with prior work of Saito et al.[29] on silicon surfaces. Calculated acceptor levels for 1-dodecene and dodecane lie at energies higher than vacuum, whereas TFAAD and its saturated analog have acceptor levels below vacuum;[8,15] hence, a 1-dodecene layer is expected to appear brighter than a TFAAD layer or a TFAAD/dodecene layer.[15] These results strongly suggest that the bright edge in the SEM image in Figure 5d arises from a narrow region consisting almost exclusively of 1-dodecene molecules, originating from the original boundary defined by TFAAD patterns and extending into the region that was H-terminated. The bright edge thickness, therefore, offers an excellent estimate of the lateral growth of the 1-dodecene layer over the course of a 15 h reaction. It is important to note that growth of the 1-dodecene layer in the lateral direction (parallel to the surface plane) is much faster than growth perpendicular to the surface; the grafted 1-dodecene layer extends $\sim$1 μm away from the boundary of the TFAAD seed layer, but the height difference from the center of the pattern (expected to be H-terminated carbon) to the TFAAD region increases only by $\sim$1 nm after subsequent grafting of 1-dodecene or dodecane.

The above experiments demonstrate that photochemical grafting of TFAAD onto H-terminated carbon leads to sharp chemical boundaries that are visible by AFM and SEM. The patterned TFAAD molecules can be used to locally initiate the photochemical grafting of other hydrocarbons. Experiments with dodecane and 1-dodecene demonstrate that the initial TFAAD pattern is retained after a second hydrocarbon grafting. In both cases only a small increase in the height was observed. However, saturated and unsaturated molecules behave very differently in terms of the lateral growth of the organic layer. The final sharpness is strongly dependent on the specific molecule used; Figure 6 shows the proposed chemical composition and topography inferred from a combination of patterning, IRRAS, and XPS experiments. Unsaturated molecules are able to graft further away from the initially TFAAD-demarcated areas than saturated ones, and the resulting chemical composition of the organic layers is remarkably different.

4. Discussion

We recently proposed a mechanism for the photochemical functionalization of amorphous carbon using terminal alkenes in which photoemission of an electron into the liquid was a key step to initiate the reaction.[8] These earlier results showed that the interplay between the photoemission properties of the surface and the electron-accepting properties of the liquid is important for predicting the reaction efficiency. In particular, we showed that surface attachment of good electron acceptors facilitates subsequent grafting of unreactive molecules. The experimental results shown in the present work provide new insights on how this enhancement takes place. A first observation is that TFAAD reactions on amorphous carbon lead to the formation of multilayers, suggesting that electron photoemission into liquid TFAAD can take place through TFAAD molecular layers. Second, we found that photoemission can still take place when TFAAD-terminated carbon is in contact with liquids that are completely unreactive at the H-terminated surface. The chemical changes induced by the photoemission process on TFA groups and the resulting chemical structure of the final organic layer, however, are highly dependent on the liquid environment surrounding the surface-bound TFA. Third and more surprisingly, we found that the presence of surface-bound electron acceptors can enhance the grafting of molecules not only on top of TFAAD-terminated surfaces in a direction normal to the surface but also on bare H-terminated carbon adjacent to TFA groups in a direction parallel to the surface. Lateral grafting on carbon was found indeed to be much faster than normal grafting on TFAAD layers. These findings and how they relate to the mechanism of enhancement will be discussed in the following sections.

Organic Layer Thickness and Growth. Previous studies by us and by others showed that the growth of TFAAD organic layers on amorphous carbon and on diamond surfaces is self-terminating unless reactions are carried out over very long times of $>15-20$ h;[4,5,8] AFM data presented here demonstrates that on amorphous carbon self-termination occurs at a molecular thickness of approximately 5 nm (corresponding to $\sim$3 molecular layers). This thickness is consistent with our proposed TFAAD grafting mechanism in which electron photoemission from the substrate into molecular levels of TFAAD initiates the reaction. A 5 nm thickness is in fact approximately 3 times the reported attenuation depth for the transmission of low-energy photoelectrons ($<$1.5 eV) through hydrocarbon films, typically found in the range 0.7$-$2 nm.[30$-$32] Only $\sim$5% of photoemitted electrons could therefore be transmitted once the TFAAD layer self-terminates leading to a consequent reduction of the grafting rate. Our results indicate that indeed functionalization occurs most rapidly during an initial phase, during which UV irradiation readily creates radicals adjacent to the surface via internal photoemission of electrons into the liquid TFAAD adjacent to the surface. After the formation of TFAAD multilayers, grafting is still possible, but the rate at which radical anions are generated is much slower because photoemission into acceptor levels either in the liquid or chemisorbed on the surface must occur through the molecular layer. Similarly, any counter-reactions that preserve charge neutrality must occur not on bare carbon but on/through a TFAAD multilayer.

TFAAD Photodegradation. Our IRRAS and XPS data both indicate that TFA groups undergo fragmentation during photochemical grafting. However, it is important to identify whether

this fragmentation is a necessary component of the reaction mechanism or if it is merely a side-reaction. Surprisingly, the rate at which the TFA groups are degraded depends strongly on the nature of the hydrocarbon in contact with the surface. The half-life of the C−F bond can be estimated from the curves in Figure 2b to be 2.6 h in vacuum and 9.8 h in dodecane, whereas in 1-dodecene the C−F cleavage rate is so slow that it was not possible to determine a half-life value over the course of 15 h reactions. Our data also show that 1-dodecene also grafts more readily than dodecane. Thus, the simple presence of the unsaturated bond in 1-dodecene significantly improves the stability of the surface-bound TFA group and also improves the efficacy of grafting of the hydrocarbon. From this, we conclude that photodegradation of the TFA group is not a requirement for the subsequent covalent grafting of saturated or unsaturated hydrocarbons to take place but is simply a byproduct of the photoemission process.

This stabilizing effect associated with a single unsaturated C═C bond cannot be explained solely on the basis of thermal or dielectric properties of the liquids. Thermal decomposition of organohalides typically occurs through cleavage of the C−X bond, but such processes occur at relatively high temperatures (>200 °C),[33,34] which can be excluded in our experiments with 1-dodecene and dodecane and can likely be excluded even in vacuum. Moreover, the striking difference in stability of the TFA groups when in contact with dodecane and 1-dodecene cannot be explained in terms of their ability to dissipate heat since *n*-alkane and *n*-alkene analogs display similar thermal properties.[35,36] While the dielectric properties of solvents modulate radical/ion electrostatic interactions and are known to modify the kinetics of organohalide dissociative charge-transfer reactions,[37−39] dodecane and 1-dodecene have nearly identical dielectric constants of 2.01 and 2.15, respectively.[40] Thus, the differences between 1-dodecene and dodecane are not easily ascribed to differences in thermal or dielectric properties.

We believe the increased stability of the TFA groups in contact with 1-dodecene likely arises from the differences in electron affinities of dodecane and 1-dodecene. Calculated gas-phase EAs of 1-dodecene and dodecane place their affinity levels at −2.29[8] and −4.19 eV,[15] corresponding to acceptor levels at +2.29 and +4.19 eV above vacuum, respectively. In the liquid phase, these acceptor levels are stabilized by a solvation energy contribution also known as Born energy;[41] assuming a typical Born energy value of ∼1.5 eV,[42] the acceptor levels of 1-dodecene and dodecane would be placed at ∼0.8 and 2.7 eV above the vacuum level, respectively. Our UPS data show a work function of 3.2 eV on TFAAD-modified carbon in vacuum; a 4.9 eV photon source should therefore be able to transfer electrons into acceptor levels lying up to ∼1.7 eV above the vacuum level.[8] Thus, electron transfer to 1-dodecene should be facile, while transfer to dodecane should be much more difficult.

Electron attachment to trifluoroacetamides and organohalides in general is known to lead to dissociation into radical and ionic fragments, as shown by radiolysis,[20−22,43,44] electrochemical, and photoelectrochemical experiments.[45−50] We propose that $TFA^{-\bullet}$ groups can fragment via C−F bond cleavage in a manner similar to the behavior of organohalide radical anions. The photodegradation data suggest that two possible photochemical pathways exist, as shown in Figure 7: (a) photoinduced electron transfer to surface-bound TFA takes place and the resulting $TFA^{-\bullet}$ decays through fragmentation and (b) hydrocarbons (1-dodecene) in the liquid are able to accept photoemitted electrons and dissipate the charge away from the surface. Pathway (b) would compete with (a), thus explaining the reduced fragmentation rates observed in 1-dodecene. The fast photodegradation of the C−F bonds in vacuum then can be viewed as an extreme case in which no charge dissipation is possible after forming the $TFA^{-\bullet}$, and only the dissociative decay channel is available to charged TFA moieties.

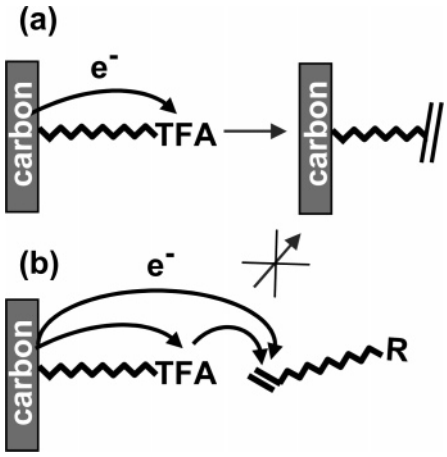

Figure 7. Schematic describing two competing pathways in photoinduced electron transfer from carbon to the organic phase. (a) Photoinduced reduction to $TFA^{-\bullet}$ and subsequent fragmentation. (b) Photofragmentation is avoided because the negative charge is transferred to acceptors in the liquid.

Chemical Contrast and Covalent Grafting Mechanism. Understanding the factors controlling the overall photochemical grafting of molecular layers to surfaces is complicated by the fact that photoexcitation creates both electrons and holes. While individual steps in the grafting reactions may involve oxidation or reduction reactions, under steady-state conditions the rate of these must be equal. Consequently, the overall rate of the covalent grafting process is not necessarily controlled by the grafting reaction, but possibly by other reactions necessary to maintain charge neutrality.

Nichols et al.[14] and Wang et al.[15] recently reported on the possibility of patterning hydrogen-terminated diamond with photochemical methods. Those results showed that sharp patterns could be obtained using TFAAD on nanocrystalline diamond, but on single-crystal diamond the transition from functionalized to nonfunctionalized regions was more diffuse. This broadened transition region was attributed to the fact that the photoemission creates holes in the valence band, and that these holes can diffuse laterally more easily on single-crystal diamond than on nanocrystalline diamond. Our present results show that chemical patterns can also be created on amorphous carbon with sharp transitions of ∼0.3 μm or less between functionalized and nonfunctionalized regions; this width is consistent with the expected diffraction-limited excitation profile at the surface.[15] The presence of such sharp transition regions shows that diffusion of radical species in the liquid or charge delocalization in the carbon substrate do not significantly affect the spatial resolution during grafting of TFAAD. However, our results also show that subsequent photochemical reactions using TFAAD as a "seed" layer to enhance the reactivity can preserve the sharpness (as with dodecane) or can lead to substantial loss in sharpness (as with 1-dodecene). This effect is clear in the case of 1-dodecene, where the pregrafting of TFAAD causes enhanced grafting over a region ∼3 μm wide. The phase contrast in AFM and the enhanced brightness of the pattern edges observed with SEM for this sample are consistent with a

1-dodecene reaction front that originates from TFAAD edges (see Figure 6).

To understand how TFAAD pregrafting enhances the local reactivity toward 1-dodecene, we note that photoemission of electrons into the liquid phase creates radical species in the liquid and positive charges (holes) in the amorphous carbon substrate, both of which can possibly impact the reaction. Additionally, previous experiments with photochemical grafting of alkenes onto silicon suggest that the possibility of radical propagation steps must be addressed.

A key piece of experimental data is that when grafting 1-dodecene onto the TFAAD-patterned surface, the dodecene forms a molecular layer approximately $\sim 3\ \mu$m in width adjacent to the TFAAD regions, but this reaction does not appreciably change the height difference between the H- and the TFAAD-terminated regions. Thus, grafting onto the H-terminated carbon adjacent to TFAAD is faster than covalent attachment on top of the TFAAD layer. Previous studies of styrene and 1-decene chemisorption onto H-terminated silicon showed that bonding of one molecule to the surface resulted in a molecular radical that could abstract a hydrogen atom from adjacent Si−H bonds, thus creating a new surface adsorption site; this process could then repeat, leading to a radical propagation process on the surface.[51−53] However, in all of these cases the surface propagation front does not extend beyond 5 nm from the initial surface radical site, thus suggesting that it is unlikely that a similar surface propagation can account for the $\sim 3\ \mu$m width transition region observed in our experiments. Previous studies have also used UV-initiated creation of surface-bound radical initiators to form polymerized layers on sufaces.[54−56] In these cases, however, the polymerization primarily induces an increase in the thickness of the layer, as polymerization occurs on top of the radical initiation site. In contrast, in our studies we observed an increase in reaction adjacent to the TFAAD layer. Simple radical chain propagation is therefore not likely to be an important factor controlling the lateral growth on the "seeded" surfaces. Instead, the overall reaction must be limited by a chemical reaction step at the H-terminated carbon surface. The two most likely processes controlling the propagating reaction front are (1) diffusion of radicals in the liquid-phase that abstract H atoms from the adjacent H-terminated surface regions and (2) diffusion of holes within the amorphous carbon that enhance reactivity by increasing the nucleophilicity of the adjacent surface.

In the first mechanism, liquid-phase radicals could enhance grafting on the surface by abstracting surface H atoms, creating surface radical sites that can add to olefin groups of other molecules in the liquid phase. Previous studies have shown that radical species such as benzoyl peroxide can initiate grafting of molecular layers onto H-terminated diamond samples by abstraction of the surface H atoms.[57−59] Similar processes may then be expected to occur for photochemically generated radicals on H-terminated amorphous carbon. Because TFAAD lowers the work function and enhances the local emission of electrons, the concentration of liquid-phase reactive species would be expected to be higher in the TFAAD-modified regions. If radical species generated in proximity of TFAAD-terminated regions had sufficiently long lifetimes, they could diffuse from the site of their formation, thus enhancing grafting on regions adjacent to TFAAD molecules. Diffusion coefficients of hydrocarbon radical species typically are in the range $0.5-1.0 \times 10^{-5}$ cm^2/s,[60−62] so that the required lifetime of a radical to span a 1 μm distance would need to be at least 10^{-3} s. While radical lifetimes are typically shorter than this due to radical−radical termination reactions,[63] one would expect that at very low concentrations the radicals may be able to diffuse this distance.

In the second possible mechanism, the local enhancement may be controlled by the fact that because TFAAD facilitates electron photoemission, the surface regions under the TFAAD layer also have a higher concentration of holes. The diffusion of holes from the TFAAD-terminated region into the immediately adjacent nonfunctionalized regions may enhance the reactivity of the latter in a manner similar to that proposed previously for the photoinitiated grafting of alkenes to silicon surfaces,[64,65] in which valence-band holes make the surface more electrophilic and thereby increase its reactivity toward electron-rich olefins. In a recent study, we found that patterned photochemical grafting of TFAAD on single-crystal diamond yielded a broad transition region while an identical experiment on nanocrystalline diamond yielded a sharp chemical pattern,[15] and we suggested that the diffusion of holes may be important. Our present results on amorphous carbon reinforce this picture: the lifetime of photogenerated charge carriers in amorphous carbon can be very long, up to the millisecond range, and diffusion lengths have been estimated to be up to $\sim$700 nm,[66−68] consistent with the width of the observed 1-dodecene reaction front.

Both of the above processes have the potential to enhance the reaction rate at the H-terminated carbon surface adjacent to TFAAD-terminated regions. To explain the wider transition region observed for 1-dodecene compared with dodecane, we note that the XPS data show reduced degradation of TFA in contact with 1-dodecene; this implies that 1-dodecene is a better electron acceptor, and that more photoelectron ejection (and hence, more holes) occur with 1-dodecene than with dodecane. Thus, higher local concentrations of both radical species in the liquid and holes in the solid would be expected in the TFAAD-terminated regions in the case of 1-dodecene. Diffusion of a larger number of either holes in the solid or radicals in the liquid would be consistent with an enhanced reactivity away from the TFAAD-terminated regions for 1-dodecene versus dodecane.

5. Conclusions

We have investigated the mechanism by which TFAAD layers can modulate the photochemical reactivity of a carbon-based semiconductor. The electronic structure of the chemisorbed layer plays an important role in promoting the reactivity at carbon/organic interfaces. The attractive electron affinity of TFA groups facilitates electron capture and charge transfer into the liquid phase.

Photodegradation and photoemission results show that an electron-driven process is at the origin of the enhanced reactivity of TFAAD-modified carbon. While photoemission of an electron is necessary to drive the functionalization, the photodegradation results suggest that the electron does not necessarily need to be captured by the TFA group in order for the reaction to proceed. Our results suggest that the most important role of surface-bound TFA groups is to increase the photoemission yield; consequently, we anticipate that there are likely other molecular groups that can enhance electron emission and promote reactivity.

An important implication of these findings is that, while electron photoemission is necessary on amorphous carbon, the resulting holes may also play an important role in controlling the overall spatial distribution and kinetics of grafting. Previous studies on silicon suggested an excitonic mechanism in which organic olefins interacted with the valence band hole.[64,65] Recent work on diamond and amorphous carbon showed that grafting

is initiated via an internal photoemission process.[4,8] Our work here on amorphous carbon suggests that one common feature of all these systems is the photoinitiated creation of a valence band hole with differences arising primarily in the manner in which this hole is created: either via absorption of light in the bulk and creation of a bulk electron−hole pair (as in the excitonic mechanism for silicon) or via direct excitation of electrons directly from the surface into the adjacent fluid (internal photoemission), as we observe here for amorphous carbon.

We note that while the "hole" mechanism provides an intriguing way of unifying the photochemical grafting observed on different surfaces, our results are not able to definitively identify whether the spatial resolution of grafting is controlled by diffusion of holes or by diffusion of reactive species in the liquid phase. The presence of a molecular mediator such as TFAAD locally enhances the photoemission of electrons into the adjacent fluid and therefore also increases the local concentration of holes. Ultimately, the requirements of charge neutrality suggest that the presence of both electrons and holes may be necessary to permit grafting under steady-state conditions.

Electron photoemission emerges from these experiments as a mechanism for semiconductor functionalization; an alternative route that becomes available through the choice of suitable incident energy and electron acceptors at the semiconductor/organic interface. The use of a molecular mediator in controlling charge transfer at the semiconductor/organic interface offers a practical approach to the functionalization of semiconducting materials and nanomaterials and at the same time reveals the importance of solid/molecule electronic interactions in determining the photochemical reactivity of functional surfaces.

Acknowledgment. This manuscript is based on research supported by the National Science Foundation Grant CHE-0613010 and DMR-0520527.

Supporting Information Available: IRRAS of control grafting reactions between hydrogen-terminated carbon and dodecane and 1-dodecene. This information is available free of charge via the Internet at http://pubs.acs.org.

References and Notes

(1) Yang, W. S.; Auciello, O.; Butler, J. E.; Cai, W.; Carlisle, J. A.; Gerbi, J.; Gruen, D. M.; Knickerbocker, T.; Lasseter, T. L.; Russell, J. N., Jr.; Smith, L. M.; Hamers, R. J. *Nat. Mater.* **2002**, *1*, 253.

(2) Sun, B.; Colavita, P. E.; Kim, H.; Lockett, M.; Marcus, M. S.; Smith, L. M.; Hamers, R. J. *Langmuir* **2006**, *22*, 9598.

(3) Strother, T.; Knickerbocker, T.; Russell, J. N., Jr.; Butler, J. E.; Smith, L. M.; Hamers, R. J. *Langmuir* **2002**, *18*, 968.

(4) Nichols, B. M.; Butler, J. E.; Russell, J. N., Jr.; Hamers, R. J. *J. Phys. Chem. B* **2005**, *109*, 20938.

(5) Yang, N.; Uetsuka, H.; Watanabe, H.; Nakamura, T.; Nebel, C. E. *Chem. Mater.* **2007**, *19*, 2852.

(6) Nebel, C. E.; Shin, D.; Takeuchi, D.; Yamamoto, T.; Watanabe, H.; Nakamura, T. *Diamond Relat. Mater.* **2006**, *15*, 1107.

(7) Härtl, A.; Schmich, E.; Garrido, J. A.; Hernando, J.; Catharino, S. C. R.; Walter, S.; Feulner, P.; Kromka, A.; Steinmuller, D.; Stutzmann, M. *Nat. Mater.* **2004**, *3*, 736.

(8) Colavita, P. E.; Sun, B.; Tse, K.-Y.; Hamers, R. J. *J. Am. Chem. Soc.* **2007**, *129*, 13554.

(9) Baker, S. E.; Tse, K. Y.; Hindin, E.; Nichols, B. M.; Clare, T. L.; Hamers, R. J. *Chem. Mater.* **2005**, *17*, 4971.

(10) Yu, S. S. C.; Downard, A. J. *Langmuir* **2007**, *23*, 4662.

(11) Baker, S. E.; Colavita, P. E.; Tse, K. Y.; Hamers, R. J. *Chem. Mater.* **2006**, *18*, 4415.

(12) Metz, K. M.; Goel, D.; Hamers, R. J. *J. Phys. Chem. C* **2007**, *111*, 7260.

(13) Metz, K. M.; Tse, K. Y.; Baker, S. E.; Landis, E. C.; Hamers, R. J. *Chem. Mater.* **2006**, *18*, 5398.

(14) Nichols, B. M.; Metz, K. M.; Tse, K. Y.; Butler, J. E.; Russell, J. N., Jr.; Hamers, R. J. *J. Phys. Chem. B* **2006**, *110*, 16535.

(15) Wang, X.; Colavita, P. E.; Metz, K. M.; Butler, J. E.; Hamers, R. J. *Langmuir* **2007**, *23*, 11623.

(16) Tolstoy, V. P.; Chernyshova, I.; Skryshevsky, V. A. *Handbook of Infrared Spectroscopy of Ultrathin Films*; John Wiley & Sons: New York, 2003.

(17) Shirley, D. A. *Phys. Rev. B* **1972**, *5*, 4709.

(18) Moulder, J. F.; Stickle, W. F.; Sobol, P. E.; Bomben, K. D. *Handbook of X-ray Photoelectron Spectroscopy*; Perkin-Elmer Corporation: Eden Prairie, MN 1992.

(19) Barrow, G. M. *Introduction to Molecular Spectroscopy*; McGraw-Hill: New York, 1962.

(20) Chen, T. C. S.; Kispert, L. D. *J. Chem. Phys.* **1976**, *65*, 2763.

(21) Rogers, M. T.; Kispert, L. D. *J. Chem. Phys.* **1967**, *46*, 3193.

(22) Samskog, P.-O.; Kispert, L. D. *J. Chem. Phys.* **1983**, *78*, 2129.

(23) Schlaf, R.; Schroeder, P. G.; Nelson, M. W.; Parkinson, B. A.; Lee, P. A.; Nebesny, K. W.; Armstrong, N. R. *J. Appl. Phys.* **1999**, *86*, 1499.

(24) Ertl, G.; Küppers, J. *Low-Energy Electrons and Surface Chemistry*; Wiley-VCH: Weinheim, 1986.

(25) Noy, A.; Sanders, C. H.; Vezenov, D. V.; Wong, S. S.; Lieber, C. M. *Langmuir* **1998**, *14*, 1508.

(26) Hayashi, K.; Sugimura, H.; Takai, O. *Appl. Surf. Sci.* **2002**, *188*, 513.

(27) Cazaux, J. *J. Microsc.* **2004**, *214*, 341.

(28) Seiler, H. *J. Appl. Phys.* **1983**, *54*, R1.

(29) Saito, N.; Wu, Y.; Hayashi, K.; Sugimura, H.; Takai, O. *J. Phys. Chem. B* **2003**, *107*, 664.

(30) Chang, Y. C.; Berry, W. B. *J. Chem. Phys.* **1974**, *61*, 2727.

(31) Monjushiro, H.; Watanabe, I. *Anal. Sci.* **1995**, *11*, 797.

(32) Cartier, E.; Pfluger, P.; Pireaux, J. J.; Vilar, M. R. *Appl. Phys. A* **1987**, *44*, 43.

(33) Egger, K. W.; Cocks, A. T. Pyrolysis reactions involving carbon-halogen bonds. In *The chemistry of carbon-halogen bond*; Patai, S., Ed.; John Wiley & Sons: Bristol, 1973; Vol. 2; pp 677.

(34) Kim, C. S.; Mowrey, R. C.; Butler, J. E.; Russell, J. N. *J. Phys. Chem. B* **1998**, *102*, 9290.

(35) Watanabe, H.; Hideyuki, K. *J. Chem. Eng. Data* **2004**, *49*, 809.

(36) Watanabe, H.; Seong, D. J. *Int. J. Thermophys.* **2002**, *23*, 337.

(37) Bertran, J.; Gallardo, I.; Moreno, M.; Savéant, J. M. *J. Am. Chem. Soc.* **1992**, *114*, 9576.

(38) Cardinale, A.; Isse, A. A.; Gennaro, A.; Robert, M.; Savéant, J. M. *J. Am. Chem. Soc.* **2002**, *124*, 13533.

(39) Pause, L.; Robert, M.; Savéant, J. M. *J. Am. Chem. Soc.* **2001**, *123*, 11908.

(40) *CRC Handbook of Chemistry and Physics*, 86th ed.; Lide, D. R., Ed.; CRC Press: Boca Raton, FL, 2005; pp 6.

(41) Born, M. *Z. Phys. A: Hadrons Nucl.* **1920**, *1*, 45.

(42) Holroyd, R. A.; Russell, R. L. *J. Phys. Chem.* **1974**, *78*, 2128.

(43) Toriyama, K.; Iwasaki, M. *J. Phys. Chem.* **1969**, *73*, 2663.

(44) Bühler, R. E. Radiation chemistry of the carbon-halogen bond. In *The chemistry of carbon-halogen bond*; Patai, S., Ed.; John Wiley & Sons: Bristol, 1973; Vol. 2; pp 795.

(45) Andrieux, C. P.; Merz, A.; Savéant, J. M. *J. Am. Chem. Soc.* **1985**, *107*, 6097.

(46) Andrieux, C. P.; Gallardo, I.; Savéant, J. M.; Su, K. B. *J. Am. Chem. Soc.* **1986**, *108*, 638.

(47) Andrieux, C. P.; Combellas, C.; Kanoufi, F.; Savéant, J. M.; Thièbault, A. *J. Am. Chem. Soc.* **1997**, *119*, 9527.

(48) Savéant, J. M. Electron transfer, bond breaking and bond formation. In *Advances in Physical Organic Chemistry*; Tidwell, T. T., Ed.; Academic Press: San Diego, CA, 2000; Vol. 35; pp 117.

(49) Hawley, M. D. In *Encyclopedia of electrochemistry of the elements*; Bard, A. J., Lund, H., Eds.; Marcel Dekker: New York, 1980; Vol. XIV.

(50) Casanova, J.; Eberson, L. Electrochemistry of the carbon-halogen bond. In *The chemistry of carbon-halogen bond*; Patai, S., Ed.; John Wiley & Sons: Bristol, 1973; Vol. 2; pp 979.

(51) Lopinski, G. P.; Wayner, D. D. M.; Wolkow, R. A. *Nature* **2000**, *406*, 48.

(52) Cicero, R. L.; Chidsey, C. E. D.; Lopinski, G. P.; Wayner, D. D. M.; Wolkow, R. A. *Langmuir* **2002**, *18*, 305.

(53) Eves, B. J.; Sun, Q. Y.; Lopinski, G. P.; Zuilhof, H. *J. Am. Chem. Soc.* **2004**, *126*, 14318.

(54) Prucker, O.; Ruhe, J. *Langmuir* **1998**, *14*, 6893.

(55) Schmidt, R.; Zhao, T. F.; Green, J. B.; Dyer, A. J. *Langmuir* **2002**, *18*, 1281.

(56) Kaholek, M.; Lee, W. K.; Feng, J. X.; LaMattina, B.; Dyer, D. J.; Zauscher, S. *Chem. Mater.* **2006**, *18*, 3660.

(57) Tsubota, T.; Hirabayashi, O.; Ida, S.; Nagoka, S.; Nagata, M.; Matsumoto, Y. *Diamond Relat. Mater.* **2002**, *11*, 1360.

(58) Ida, S.; Tsubota, T.; Tanii, S.; Nagata, M.; Matsumoto, Y. *Langmuir* **2003**, *19*, 9693.

(59) Tsubota, T.; Tanii, S.; Ida, S.; Nagata, M.; Matsumoto, Y. *Diamond Relat. Mater*. **2004**, *13*, 1093.
(60) Terazima, M. *Acc. Chem. Res.* **2000**, *33*, 687.
(61) Burkhart, R. D.; Boynton, R. F.; Merrill, J. C. *J. Am. Chem. Soc.* **1971**, *93*, 5013.
(62) Burkhart, R. D. *J. Am. Chem. Soc.* **1973**, *95*, 7203.
(63) Togo, H. What are free radicals? In *Advanced free radical reactions for organic synthesis*, 1st ed.; Elsevier, Ltd.: Amsterdam, 2004; pp 1.
(64) Stewart, M. P.; Buriak, J. M. *J. Am. Chem. Soc.* **2001**, *123*, 7821.
(65) Sun, Q.-Y.; de Smet, L. C. P. M.; van Lagen, B.; Giesbers, M.; Thüne, P. C.; van Engelenburg, J.; de Wolf, F. A.; Zuilhof, H.; Sudhölter, E. J. R. *J. Am. Chem. Soc.* **2005**, *127*, 2514.
(66) Dluzniewski, M.; Kania, S. *Diamond Rel. Mater*. **2005**, *14*, 74.
(67) Staryga, E.; Bak, G. W. *Diamond Rel. Mater*. **2005**, *14*, 23.
(68) Bak, G. W.; Dluzniewski, M.; Staryga, E.; Kania, S.; Walocha, J. *Diamond Rel. Mater*. **2000**, *9*, 1357.